DOI: 10.1002/cbdv.202000083

FULL PAPER

CHEMISTRY & BIODIVERSITY

Multi-Targeting Tacrine Conjugates with Cholinesterase and Amyloid-Beta Inhibitory Activities: New Anti-Alzheimer's Agents

Asha Hiremathad,[a, b] Sílvia Chaves,[b] and Rangappa S. Keri*[a]

[a] Organic and Medicinal Chemistry Laboratory, Center for Nano and Material Sciences, Jain University, Jain Global Campus, Jakkasandra Post, Kanakapura Road, Ramanagara District, Karnataka-562112, India, e-mail: keriphd@gmail.com; sk.rangappa@jainuniversity.ac.in

[b] Centro de Química Estrutural and Departamento de Engenharia Química, Instituto Superior Técnico, Universidade de Lisboa, Av. Rovisco Pais 1, 1049-001 Lisboa, Portugal

Alzheimer's disease (AD) is a severe age dependent and chronic problem with no cure so far. The available treatments are temporary, acting over short period of time. The main pathological hallmark of the disease includes cholinergic dysfunction, oxidative stress, accumulation of Aβ fibrils and *tau* tangles. In context with the multi-factorial nature of this disease, two different series of molecules were developed to hit the multifactorial disease targets. Mainly, the molecules were designed to inhibit the AChE and aggregation of Aβ, and also oxidative damage. Two novel series of TAC-fenbufen/menbutone conjugated molecules were designed, synthesized and bio-assayed. All compounds showed inhibition capacity towards AChE, Aβ aggregation and moderate to good radical scavenging capacity. Particularly, five TAC-menbutone molecules showed improved AChE and Aβ aggregation inhibition capacity compared to TAC-fenbufen conjugated molecules. Overall, these novel series of molecules may be potential drug lead molecules in the treatment of AD.

Keywords: Alzheimer's disease, tacrine, acetylcholinesterase inhibitors, Aβ self-aggregation inhibitors.

Introduction

Alzheimer's disease (AD) is the most common form of dementia and chronic, progressive age-related neurodegenerative disorder. The characteristics of the disease are impaired cognition, behavioral disturbances, and memory loss, resulting in difficulties to perform regular activities. This has become a devastating problem to the society, being estimated that more than 13.2 million people will be affected from AD by 2050, and also this illness has no cure so far. It is expected that the treatment for AD and other dementia will cost over $259 billion, which could even raise up to $1.1 trillion by 2050.[1] Most of the available drugs are AChE inhibitors,[2] which are symptomatic and work over a short period of time. Thus, many researchers across the globe attempted to discover effective drugs to tackle this disease. Unfortunately, there are frequent failures due to the unclear pathogenesis and multi-factorial nature of AD.[3] Some important characteristics of AD are extracellular deposition of misfolded amyloid-β (Aβ),[4,5] and intercellular accumulation of neurofibrillary tangles (NFT)[6] due to hyperphosphorylation of the *tau* protein which are toxic materials to the neurons, leading to neuronal death. Cholinergic dysfunction also occurs,[7,8] due to the rapid hydrolysis of acetylcholine (ACh) by acetylcholinesterase (AChE). Other substantial causes for the disease growth are oxidative damage[9] and variation in the homeostasis of metal ions which enhances Aβ aggregation leading to AD development.[10–12] It has been hypothesized that the cholinergic dysfunctions, probably induced by formation of extracellular Aβ plaques and *tau* tangles, may be formed in the hippocampus and cerebral cortical areas. Similarly, it is also hypothesized that neurodegeneration may occur at the cholinergic terminal due to Aβ plaques.[13,14] However, it remains unclear whether cholinergic

Supporting information for this article is available on the WWW under https://doi.org/10.1002/cbdv.202000083

dysfunctions or Aβ plaques formation are primary events causing neuronal losses in the brain. Therefore, to tackle this disease, it is very important to focus on more than one target of AD.

In this framework, the extended research of our group has made an attempt to find out novel derivatives to treat AD.[15] Herein, we present hybrids of tacrine (TAC)-fenbufen/menbutone by using an amide linker to couple TAC with two main scaffolds, biphenyl acid and methoxy naphthalene acid, which are pharmacophore entities. The TAC was selected to endeavor the hybrids with acetylcholine inhibition (AChEI),[15,16] while the other two main moieties were introduced to improve the inhibition of Aβ self-aggregation (*Scheme 1*). Inclusion of fenbufen and menbutone moieties with adequate chain length will allow interaction with peripheral anionic site (PAS) of AChE enzyme which is at the entrance side. Eventually, these new series of compounds will improve the capacity of AChE inhibition and may delay the self-aggregation of Aβ protein. Therefore, molecular docking simulation studies were performed to select the appropriate chain length and it is evidenced a good interaction of the molecules with the targeted AChE enzyme and superimposition with the original ligand (tacrine dimer). Furthermore, the synthesized compounds were assayed for their biological properties, such as inhibition of AChE, Aβ aggregation and radical scavenging activity.

Results and Discussion

Chemistry

The designed tacrine-fenbufen (TAC-fenbufen) and tacrine-menbutone (TAC-menbutone) molecules were prepared by the synthetic route shown in *Scheme 2*. The 9-chloro-1,2,3,4-tetrahydroacridine (**3**) was prepared from commercially available anthranilic acid/substituted anthranilic acid (**1**), with cyclohexanone (**2**).[13] Further, compound **3** was treated with alkyldiamines **4a**–**4c**, using a catalytic amount of KI and phenol, to give the TAC amines **5a**–**5f**.[13] Simultaneously, synthesis of two other main entities (**8**, **11**) were carried out by substitution of alkyl acids to biphenyl (**6**) and 1-methoxynaphthalene (**10**) with succinic anhydride (**7**) correspondingly to yield fenbufen (**8**) and menbutone (**11**). Finally, TAC amine precursors **5a**–**5f** were coupled with acids (**8**, **11**), respectively, by using $T_3P \geq 50$ wt.% in ethyl acetate as a coupling reagent at inert conditions for about 12 h at room temperature (r.t.) resulting in the novel TAC-fenbufen **9a**–**9d** and TAC-menbutone **12a**–**12f** conjugated molecules.

Molecular Modeling and Docking Simulations

The strategy herein adopted proposed to develop active molecules to inhibit the targeted enzyme. The two main scaffolds fenbufen and menbutone mole-

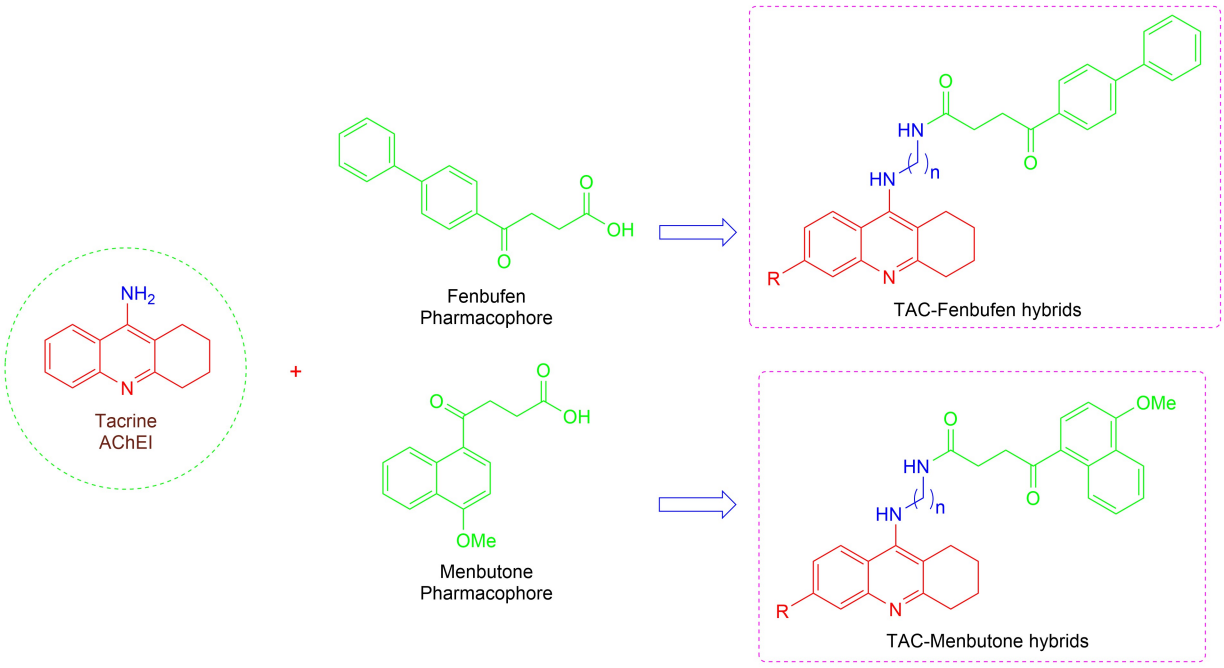

Scheme 1. Design of TAC-fenbufen and TAC-menbutone conjugates.

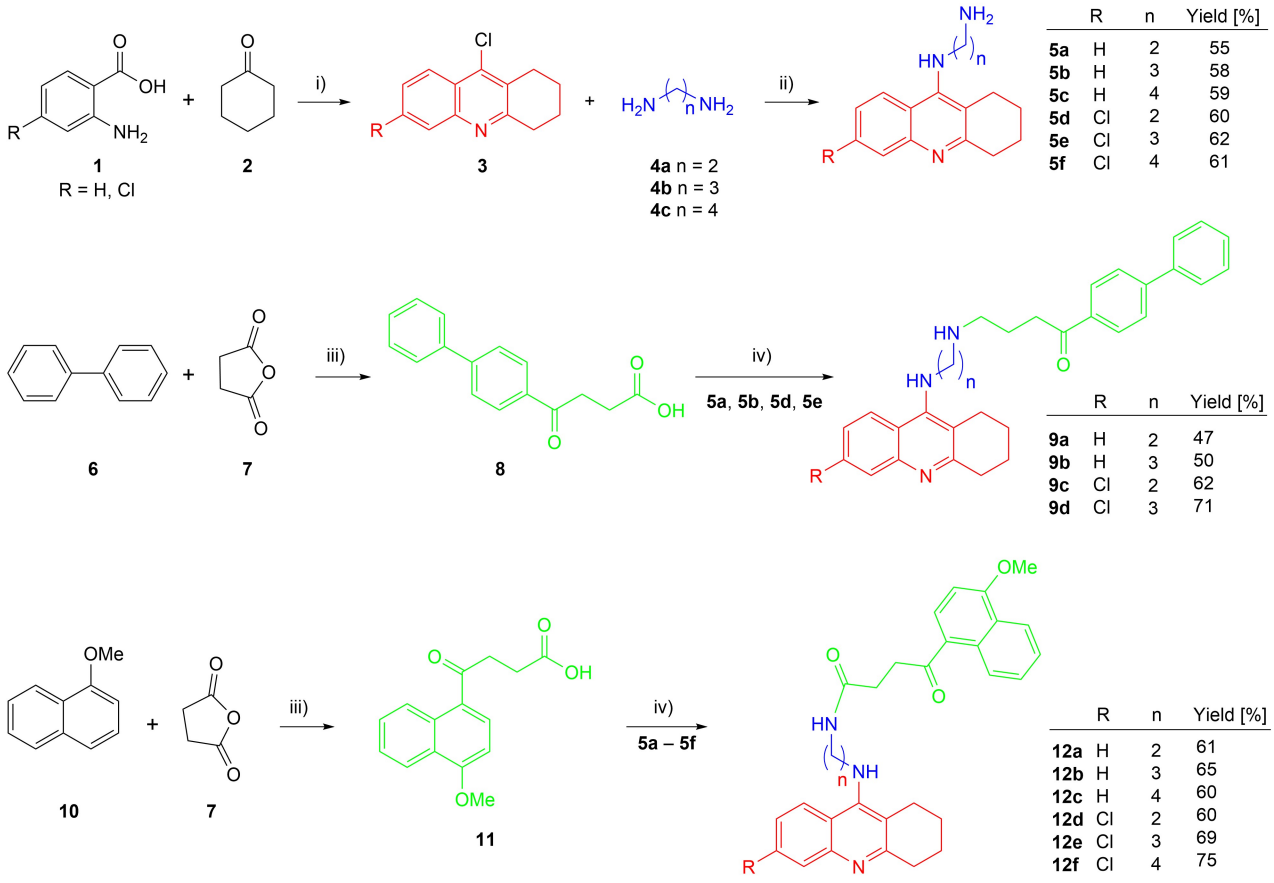

	R	n	Yield [%]
5a	H	2	55
5b	H	3	58
5c	H	4	59
5d	Cl	2	60
5e	Cl	3	62
5f	Cl	4	61

	R	n	Yield [%]
9a	H	2	47
9b	H	3	50
9c	Cl	2	62
9d	Cl	3	71

	R	n	Yield [%]
12a	H	2	61
12b	H	3	65
12c	H	4	60
12d	Cl	2	60
12e	Cl	3	69
12f	Cl	4	75

Scheme 2. Synthesis of TAC-fenbufen/menbutone conjugated molecules. Reagents and conditions: i) $POCl_3$, 180 °C, reflux, 4 h; ii) phenol, KI, 180 °C, reflux, 35 min; iii) EDC, $AlCl_3$, r.t. 4 h; iv) T_3P, NMM, DCM, N_2 atm, r.t., 12 h.

cules are pharmacophore entities, coupled with TAC. The TAC moiety was selected to assure AChE inhibition, while the other two main moieties were conjugated simultaneously to improve the inhibition of Aβ self-aggregation. Additionally, the coupling of these two moieties with an adequate linker size could improve the targeted enzyme inhibition. Therefore, the molecular simulation studies herein performed allowed in selecting the appropriate chain length. The structure obtained for this hybrid-enzyme complex is similar to the known crystal structure of *Tc*AChE complexed with (*N*-4′-quinolyl-*N*′-9″-(1″,2″,3″,4″-tetrahydroacridinyl)-1,8-diaminooctane; PDB entry 1ODC).[16] Hence, the interaction of the designed molecules with AChE was studied and compared with the original ligand 1ODC.

In the case of TAC and fenbufen hybrids, the methylene linkers $n=2$, 3 correspond to adequate chain lengths and the compound can be exactly fitted into the enzyme gorge and along that the active site; compounds **9a**–**9d** exhibited π–π stacking and interaction with the targeted enzyme in CAS and PAS showing that these designed molecules could inhibit the enzyme (*Figure 1*). The TAC moiety in the CAS side showed good π–π stacking with Trp84 and blocks of other amino acids (Ser 200, His440 and Glu327). In PAS binding site, the selected biphenyl ring is in π–π stacking with the two methylene linker ($n=2$) **9a** and **9d**, while the molecule with three methylene linker ($n=3$) chain length is quite longer than the original ligand and slightly out of PAS, even though it interacts with amino acids namely, Trp279 and Tyr70. Interestingly, most of the hybrids showed H-bonding with Tyr121 mainly, compounds **9a** and **9b** with shortest bonding distance (2.612 Å and 2.180 Å, respectively) (*Figure 1*). *In vitro* studies revealed that among all, compound **9b** ($n=3$) exhibited good inhibitory capacity towards AChE, maybe explained by the fact that the extended biphenyl ring is interacting well with the amino acid residue Tyr279. Overall, novel TAC-fenbufen conjugated molecules **9a**–**9d** are able to moderately inhibit the AChE.

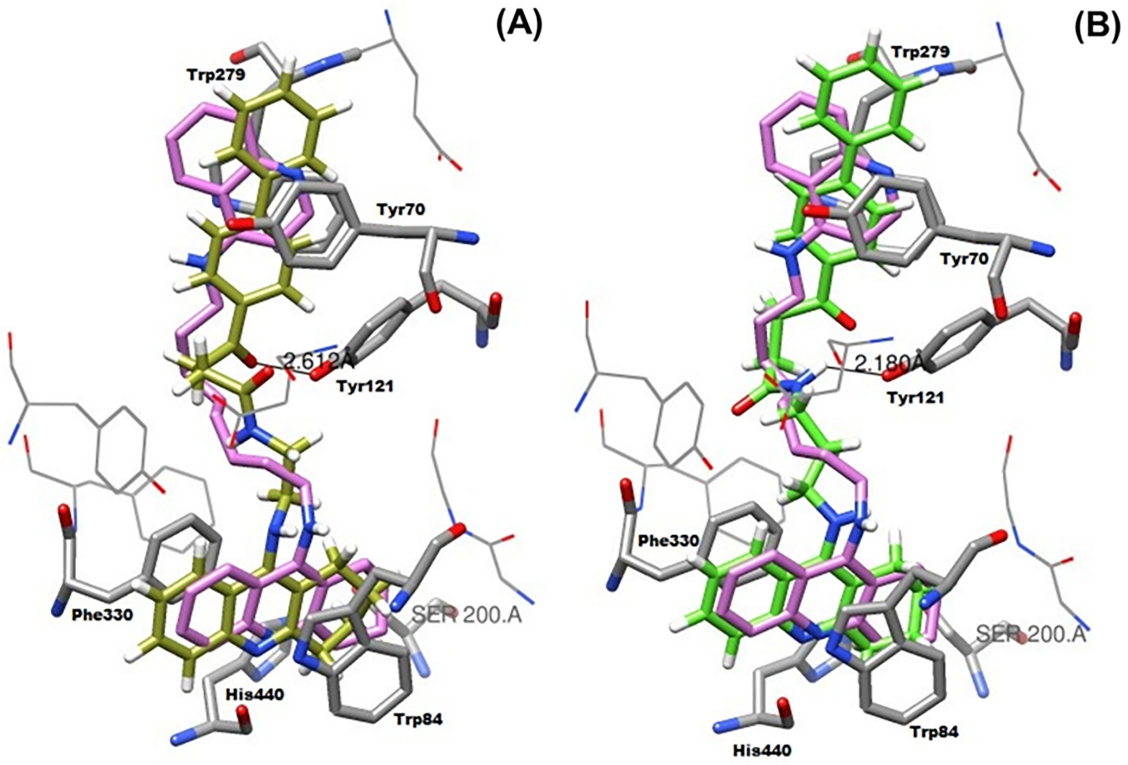

Figure 1. Docking results for the TAC-fenbufen with *Tc*AChE: (A) superimposition of **9a** (yellow) with original ligand (*N*-4′-quinolyl-*N*′-9″-(1″,2″,3″,4″-tetrahydroacridinyl)-1,8-diaminooctane; PDB entry 1ODC); (B) superimposition of **9b** (green) with original ligand.

The molecular simulations of TAC-menbutone hybrids showed that they exhibit good superimposition between the original ligand (PDB entry 1ODC) and the selected pharmacophore (menbutone), which means that the designed molecules could act as AChE inhibitors. Here, the chain length was modulated in accordance with the superimposition of the designed hybrids with the original ligand and the enzyme gorge. The docking studies showed that the designed hybrids with chain linkers ($n=2-4$) form good π–π stacking interaction with the targeted enzyme. Remarkably, the hybrids with chain linkers ($n=3$, 4) showed good interaction and adequate linker size to insert into enzyme gorge. For the molecule with the shortest linker ($n=2$, **12a**) an H-bond between carbonyl oxygen of menbutone and –OH of Tyr121 (2.056 Å) is formed. Although compounds which establish H-bonding are having usually good AChE inhibition capacity, in fact these molecules displayed low inhibition capacity in *in vitro* measurements (*Figure 2A*). For the compounds with longer linker ($n=3$) **12b** and **12e**, very good AChE inhibition capacity was exhibited, almost two fold higher than that for the parent drug tacrine. Particularly, compounds **12b** and **12e** presented the best AChE inhibition and they also exhibited good inhibition capacity towards Aβ self-aggregation (*Figure 2B,C*). In general, the docking studies provided good information between the designed drug and the targeted enzyme, which showed that the designed molecules could be able to inhibit AChE.

Pharmacokinetic Properties

To endeavor the drug-likeness of the novel compounds and their potential to penetrate important membranes such as the blood-brain barrier (BBB), some indicators of their pharmacokinetic profiles were predicted using QikProp program, v. 2.5.[17] Parameters such as the calculated octanol-water partition coefficient (*clog P*), the ability to cross the blood-brain-barrier BBB (log BB), the capacity to be absorbed through the intestinal tract to the blood (Caco-2 cell permeability) and the verification of Lipinski's rule of five, may give an idea of their drug-likeness for being orally active as anti-AD agents.[18]

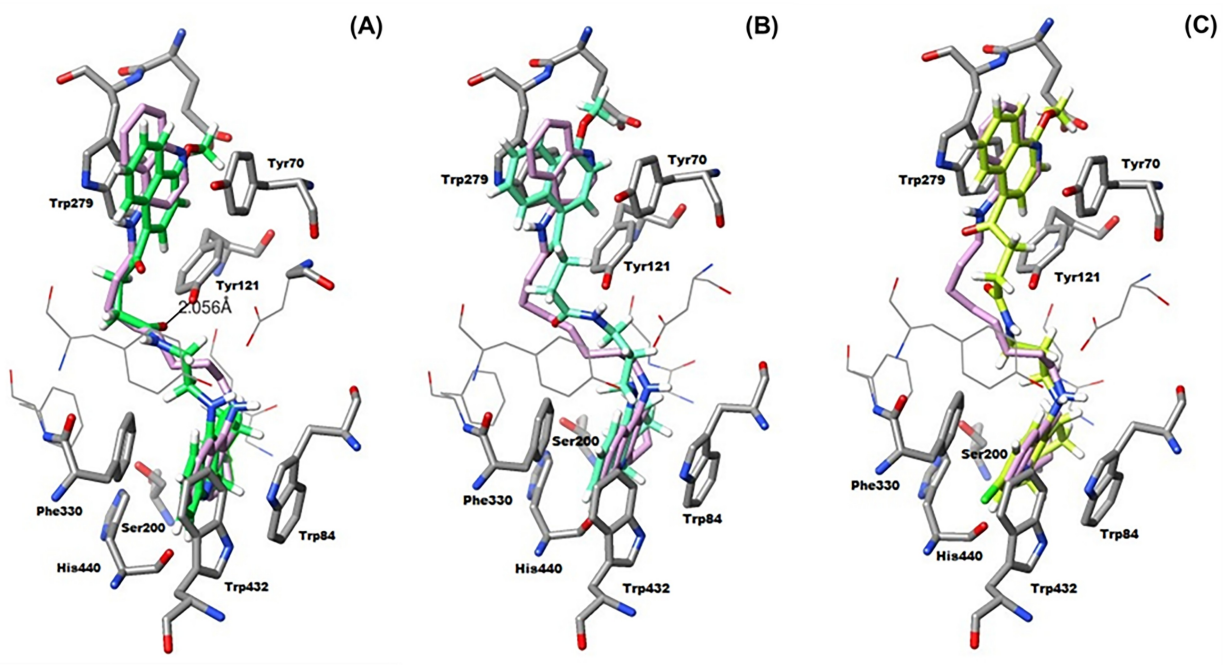

Figure 2. Docking results for the TAC-menbutone hybrids with *Tc*AChE: (A) superimposition of **12a** (green) with original ligand (*N*-4′-quinolyl-*N*′-9″-(1″,2″,3″,4″-tetrahydroacridinyl)-1,8-diaminooctane; PDB entry 1ODC); (B) superimposition of **12b** (cyan) with original ligand; (C) superimposition of **12e** (yellow) with original ligand.

Newly designed tacrine-fenbufen and tacrine-menbutone conjugated hybrids were studied for drug likeliness *in silico* by using QikProp v. 2.5.[17] The compounds have zero to two violations of Lipinski rule.[18] Namely, compound **12a** has zero violations and most of the compounds have one to two violations due to the higher value of molecular weight ($\geq$500 g/mol) and lipo-hydrophilic character ($>$5) according to the Lipinski rule.[18] Interestingly, the designed molecules have good value of logBB and Caco-2. This indicates that these compounds can pass through blood brain barrier and have good ability to be absorbed through the intestinal tract to the blood. Values of Caco-2 permeability $>$500 are considered good values for cell permeability, and the herein studied compounds have shown values in the range 591 to 1046 nm/s (*Table 1*). As a conclusion, it can be stated that these designed molecules have shown promising results for drug likeliness and therefore, it can be predicted that they are orally active agents.

Table 1. Summary of the calculated pharmacokinetic descriptors.

Compound	MW	clogP[a][b]	log BB[a][c]	Caco-2 Permeability (nm/s)[a]	CNS[a] activity	Violations of Lipinski rule[a]
9a	477.60	5.299	−0.949	833	−	1
9b	491.63	5.875	−1.353	649	−	1
9c	512.05	4.949	−0.540	911	+/−	1
9d	526.07	6.374	−0.784	1015	−	2
12a	481.59	4.181	−0.870	854	−	0
12b	516.03	5.684	−1.116	661	−	2
12c	509.64	5.263	−1.216	591	−	2
12d	516.03	5.684	−1.116	661	−	2
12e	530.06	4.755	−0.532	1010	+/−	1
12f	544.09	5.548	−0.889	1046	−	2

[a]Predicted values using program Qikprop v.2.5. [b]Calculated octanol/water partition coefficient. [c]Brain/blood partition coefficient.

Radical Scavenging Capacity

Two series of molecules were screened for their radical scavenging (RS) capacity by DPPH method.[19] This method was based on the radical scavenging capacity of molecules and interaction with DPPH free radical. Firstly, TAC-fenbufen hybrids **9a**–**9d** results revealed a moderate scavenging capacity (EC_{50} = 400 to 745 μM). However, compound **9d** showed the highest RS capacity (EC_{50} = 400 μM). Furthermore, TAC-menbutone hybrids **12a**–**12f** were tested for radical scavenging capacity and better results were obtained for RS capacity (EC_{50} = 220 to 452 μM). Mainly, compound **12b** exhibited the best RS capacity (EC_{50} = 220 μM). The methoxy substitution improved the RS capacity of the molecules. Overall, these two series of newly studied molecules displayed moderate to good radical scavenging capacity by DPPH method.

Biological Studies

AChE inhibition. Newly synthesized two series of molecules **9a**–**9d** and **12a**–**12f** are evaluated for inhibition of *Tc*AChE by a previously described method.[20,21] The IC_{50} values for inhibition of AChE are presented in *Table 2*. TAC-fenbufen hybrids **9a**–**9d**, showed good AChE inhibition, although few showed better inhibitory capacity than the parent drug TAC. Compound **9b** showed the highest inhibition (IC_{50} = 0.34 μM). Especially, compounds with a longer methylene linker (n = 3) showed improved inhibition capacity than those with the smaller chain linker (n = 2), which may be due to the better accommodation in the enzyme active site and extended biphenyl ring interaction with amino acid residue Tyr279 in PAS (*Figure 1*).

Further, TAC-menbutone hybrids **12a**–**12f** showed two fold more inhibitory capacity than TAC. In fact, compounds **12b** (IC_{50} = 0.12 μM) and **12e** (IC_{50} = 0.18 μM) showed the highest inhibitory capacity among these two series of hybrids. These two compounds **12b** and **12e** contain a three methylene linker (n = 3) and showed the best AChE inhibition which was evident from the molecular docking simulations, previewing a dual mode interaction (CAS and PAS). Specifically, the menbutone hybrids displayed better AChE inhibition, being well inserted into the enzyme gorge, and establishing interactions with amino acid residues and π–π stacking, the methoxy substitution aiding in the enhancement of AChE inhibition. Compounds with a longer chain linker (n = 4) exhibited less inhibitory capacity towards AChE. However, all these newly developed hybrids showed improved AChE inhibition compared to the parent drug tacrine.

Inhibition of Self-Mediated $A\beta_{42}$ Aggregation

To study the anti-amyloidogenic capacity of these novel TAC-fenbufen and TAC-menbutone hybrid mole-

Table 2. *In vitro* activities of the TAC-fenbufen hybrids **9a**–**9d** and TAC-menbutone hybrids **12a**–**12f**: Radical scavenging capacity (DPPH), inhibition of AChE and $A\beta_{42}$ self-aggregation.

Compound	n	R	RS Capacity[a] EC_{50} μM	AChE Inhib[b] IC_{50} (μM) ± SD	$A\beta_{42}$ self-aggreg.[c] Inhibition (%)
9a	2	H	745 ± 0.14	0.42 ± 0.08	33.5 ± 1.2
9b	3	H	450 ± 0.08	0.34 ± 0.05	28.2 ± 2.2
9c	2	Cl	542 ± 0.14	0.57 ± 0.06	46.2 ± 1.4
9d	3	Cl	440 ± 0.10	0.45 ± 0.09	42.6 ± 2.8
12a	2	H	242 ± 0.16	0.28 ± 0.07	45.6 ± 0.8
12b	3	H	220 ± 0.20	0.12 ± 0.03	70.5 ± 1.2
12c	4	H	452 ± 0.12	0.32 ± 0.08	55.0 ± 1.6
12d	2	Cl	316 ± 0.32	0.22 ± 0.06	76.2 ± 1.8
12e	3	Cl	248 ± 0.20	0.18 ± 0.1	64.5 ± 2.4
12f	4	Cl	324 ± 0.18	0.28 ± 0.08	34.5 ± 0.8
Tacrine	–		> 1000	0.38 ± 0.02	22 ± 1.6
Fenbufen			> 1000	0.97 ± 0.07	Nd
Menbutone			> 1000	0.85 ± 0.08	Nd
Trolox			15.6 ± 0.2	–	Nd

[a]EC_{50} values for the DPPH assay. [b]The values are mean of five independent experiments ± SD. [c]Inhibition of self-mediated $A\beta_{42}$ aggregation (in %). The Thioflavin-T fluorescence method was used, and the measurements were carried out in the presence of an inhibitor (80 μM). The values are the mean of two independent measurements in duplicate (SEM < 10%). Nd – Not determined.

cules, the *in vitro* ThT assay was performed by a previously described method.[22,23] The studies were performed after incubation of $A\beta_{42}$ with or without ligands. The results are displayed in *Table 2* and all the compounds were able to reduce ThT fluorescence associated with Aβ fibril binding, which indicates the inhibition of the $A\beta_{42}$ self-aggregation process.

TAC-fenbufen hybrids **9a**–**9d** exhibited a moderate inhibition capacity towards $A\beta_{42}$ aggregation. Mainly, compounds with shorter methylene linker ($n=2$) and chloro substitution on TAC moiety **9c** and **9d** showed the best inhibition (up to 46% and 42%) than compounds with a longer methylene linker ($n=3$). Furthermore, TAC-menbutone conjugated molecules were also assayed for anti-Aβ aggregation capacity by ThT assay method. Interestingly, compounds **12a**–**12f** presented good inhibitory capacity towards $A\beta_{42}$ self-aggregation (45 to 76%). Compound **12d** displayed the highest inhibition of $A\beta_{42}$ aggregation (76%) and **12b** also exhibited a very good inhibition (70%). In fact, an improved percentage of inhibition of $A\beta_{42}$ aggregation was observed for the molecules which also interact well with PAS in the AChE active site. Additionally, compounds **12c** and **12e** of the same series presented moderate to good inhibition capacity (55 and 64%, respectively). Besides, no noticeable changes are observed with variations in chain length and chloro substitution. Overall, among these two novel series, TAC-menbutone hybrids displayed better inhibitory capacity for $A\beta_{42}$ aggregation than TAC-fenbufen compounds.

Possible Structure-Activity Relationship (SAR) Studies of TAC-Fenbufen/Menbutone Hybrids

Based on biological studies, herein it is predicted the possible SAR of the TAC-fenbufen hybrids: two methylene linker length ($n=2$) was appropriate and the AChE and $A\beta_{42}$ inhibition capacity improved with chloro substitution (R=Cl) and biphenyl moiety which is interacting well at PAS. Further, these exhibited moderate-good radical scavenging capacity (**9d**; $EC_{50}=440$ μM) (*Figure 3*).

It was found that in the case of the TAC-menbutone molecules, two to three methylene chain lengths are adequate to insert into the AChE enzyme gorge. However, molecules with three methylene chain length showed significant inhibition capacity towards AChE and Aβ aggregation. The TAC moiety coupled with resulted in an enhanced AChE and $A\beta_{42}$ inhibition capacity upon coupling with menbutone. Additionally, improved radical scavenging capacity was observed for the menbutone series of molecules that could be due the methoxy group (**12b**; $EC_{50}=$ 220 μM). In general, these series of molecules **12a**–**12f** exhibited improved inhibition capacity when compared to the TAC-fenbufen hybrids **9a**–**9d**.

Conclusions

Two novel series of TAC-fenbufen **9a**–**9d** and TAC-menbutone **12a**–**12f** hybrids were developed and bioassayed such as inhibition of AChE and Aβ aggregation and radical scavenging capacity against Alzheimer's disease. Firstly, TAC-fenbufen hybrids exhibited good AChE activity as reference drug tacrine. Mainly, compound **9b** showed the highest AChE inhibition ($IC_{50}=$ 0.34 μM), RS capacity was improved for these newly conjugated molecules **9b**–**9d** ($EC_{50}=450$ μM and 440 μM, respectively). Additionally, these displayed moderate capacity to inhibit the aggregates of Aβ (**9c**; 46%). Secondly, TAC-menbutone hybrids showed the best inhibitory capacity of AChE and Aβ aggregation. This may be due to the menbutone moiety and methoxy substitution is interacting well at PAS. Especially, com-

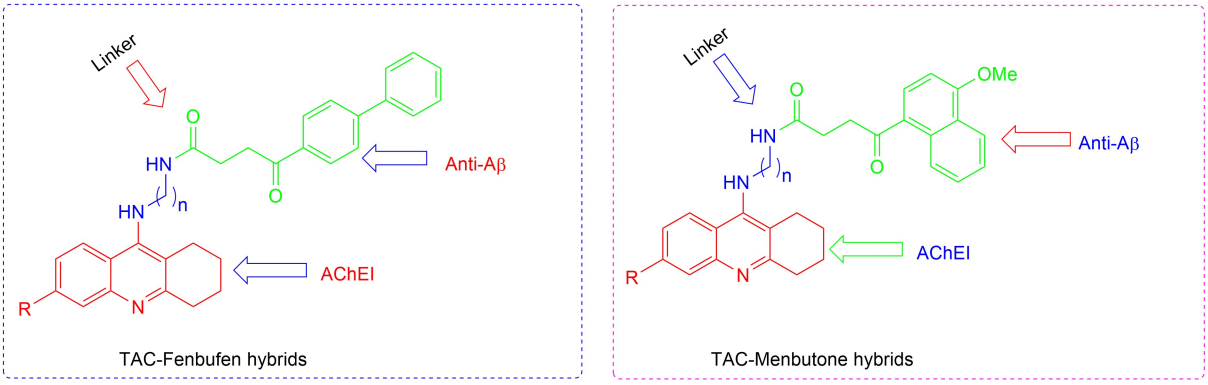

Figure 3. Possible SAR study of TAC-fenbufen/menbutone hybrids.

pounds **12b** and **12e** showed the best AChE inhibition (IC_{50} = 0.12 and 0.18 μM, respectively) which is twofold more active than the parent drug tacrine. Additionally, compounds **12b** and **12d** displayed very good inhibition of Aβ (70% and 76%, respectively). Among all, compound **12b** showed the best RS capacity (EC_{50} = 220 μM). However, among these two series of molecules TAC-menbutone hybrids showed higher activity than TAC-fenbufen hybrids. Generally, the newly synthesized exhibited moderate to good capacity of inhibition towards targeted important pathological targets and interestingly, few of the molecules **12b**, **12d**, and **12e** presented promising multi-functional activity. Hence, further study of these would leads to development of potential drugs to treat the AD.

Experimental Section

Abbreviations

AChE: acetylcholinesterase; AChEI: acetylcholinesterase inhibitors; AD: Alzheimer's disease; Aβ: amyloid-β; CAS: cationic active site; DCM: dichloromethane; DPPH: di-(phenyl)-(2,4,6-trinitrophenyl)iminoazanium; DTNB: 5,5-dithiobis(2-nitrobenzoicacid); HFIP: 1,1,1,3,3,3-hexafluoropropan-2-ol; HEPES: 2-[4-(2-hydroxy ethyl)piperazin-1-yl]ethane sulfonic acid; NFT: neurofibrillary tangles; PAS: peripheral anionic site; SAR: structure-activity relationship; TAC: tacrine; ThT: thioflavin T; T_3P: propylphosphonic anhydride solution.

General Methods and Materials

Analytical grade reagents were purchased from Sigma-Aldrich, Fluka, Alfa Aesar and Acros and were used as supplied. Solvents were dried according to standard methods.[24] The chemical reactions were monitored by TLC using alumina plates coated with silica gel 60 F_{254} (Merck). Column chromatography separations were performed on silica gel Merck 230–400 mesh (Geduran Si 60). The melting points (m.p.) were measured with a Leica Galen III hot stage apparatus and are uncorrected.[1] The ^{1}H- and ^{13}C-NMR spectra were recorded on Bruker AVANCE III spectrometers at 300 and 400 MHz, respectively. Chemical shifts (δ) are reported in ppm from the standard internal reference tetramethylsilane (TMS). Mass spectra (ESI-MS) were performed on a 500 MS LC Ion Trap (Varian Inc., Palo Alto, CA, USA) mass spectrometer equipped with an ESI ion source, operated in the positive ion mode. The electronic spectra were recorded with a PerkinElmer Lambda 35 spectrophotometer, using thermostatic 1 cm path length cells.

Molecular Modeling and Docking Simulations

To perform our docking studies the X-ray crystallographic structure of Torpedo californica-AChE (*Tc*AChE) complexed with an inhibitor was taken from RCSB Protein Data Bank (PDB entry 1ODC), in order to be used as receptor. This structure was chosen because of the similarity between its original inhibitor (*N*-4′-quinolyl-N′-9″-(1″,2″,3″,4″-tetrahydroacridinyl)-1,8-diaminooctane, PDB entry 1ODC) and our ligands: all have a tacrine moiety and an aromatic group linked through an alkyl chain. The original structure was treated using Maestro v. 9.3 by removing the original ligand, solvent, and co-crystallization molecules, and then, adding the hydrogen atoms.[25] The ligands were built using Maestro, and then, using Ghemical v. 2.0,[26] they were submitted to random conformational search (RCS) of 1000 cycles, and 2500 optimization steps using Tripos 5.2 force field.[27] The minimized ligands were docked into the AChE structure with GOLD software v. 5.1,[28] and the zone of interest was defined as the residues within 10 Å from the original position of the ligand in the crystal structure. The 'allow early termination' option was deactivated, and the remaining default parameters of Gold were used. The ligands were subjected to 100 genetic algorithm steps using ASP as fitness function.

Pharmacokinetics Properties

To analyze the drug likeliness of novel conjugated molecules as new anti-AD drugs, a brief prediction on pharmacokinetic proprieties was performed *in silico*. Parameters such as the lipo-hydrophilic character (clogP), blood-brain barrier partition coefficient (log BB), the ability to be absorbed through the intestinal tract (Caco-2 cell permeability) and CNS activity were calculated.

[1] IR characterization of the samples was not performed as the FT-IR instrument was out of service and its maintenance support was not received due the lockdown implemented during COVID-19 pandemic. However, other characterization which includes mass and NMR was performed, which confirmed the structure of the molecules.

The ligands were built and minimized as previously mentioned for the docking studies. The structures were submitted to the calculation of these relevant pharmacokinetic proprieties and descriptors using QikProp v. 2.5.[17] These predictions are for orally delivered drugs and assume non-active transport.

Radical Scavenging Capacity

The radical scavenging activity was evaluated by the DPPH method previously described.[19,29] To a 2.5 mL solution of DPPH (0.002%) in methanol, four samples of each compound in solution were added in different volumes to obtain different concentrations in a 3.5 mL final volume. The samples were incubated for 30 min at room temperature. The absorbance was measured at 517 nm against the corresponding blank (methanol). The antioxidant activity was calculated by Eqn. 1.[29]

$$\%AA = \frac{A_{DPPH} - A_{sample}}{A_{DPPH}} \times 100 \quad (1)$$

The tests were carried out in triplicate. The compound concentrations providing 50% of antioxidant activity (EC_{50}) were obtained by plotting the antioxidant activity against the compound concentration.

$$EC_{50} = \left(\frac{50 - b}{m}\right) \quad (2)$$

Where b is the interception in the y axis and m is the slope. The parameters for statistical analysis were calculated with Microsoft Office Excel®.

Biological Studies

AChE inhibition. The enzymatic activity TcAChE was measured using an adaptation of the method previously described.[20,21] The assay solution contained 374 μL of HEPES buffer (50 mM and pH 8.0), a variable volume (10–50 μL) of the stock solution of each compound in methanol (1 mg/mL), 25 μL of AChE stock solution, and the necessary amount of methanol to attain 0.925 mL of the sample mixture in a 1 mL cuvette. The samples were left to incubate for 15 min, and then, 75 μL of acetylthiocholine iodide (AChI) solution (16 mM) and 476 μL of DTNB (3 mM) were added. The reaction was monitored for 5 min at 40 nm. Assays were run with a blank containing all the components except AChE, which was replaced by HEPES buffer. The velocities of the reaction were calculated as well as the enzyme activity. A control reaction was carried out using the sample solvent (methanol) in the absence of any tested compound, and it was considered as 100% activity. The percentage inhibition of the enzyme activity due to the presence of increasing test compound concentration was calculated by the following Eqn. 3.

$$\%I = 100 - \left(\frac{V_i}{V_0} \times 100\right) \quad (3)$$

where v_i is the initial reaction rate in the presence of inhibitor and v_0 is the initial rate of the control reaction. The inhibition curves were obtained by plotting the percentage of enzymatic inhibition versus inhibitor concentration, and a calibration curve was obtained from which the linear regression parameters were obtained.

$$IC_{50} = \left(\frac{50 - b}{m}\right) \quad (4)$$

Where b is the interception in the y axis and m is the slope. The statistical analysis was performed in Microsoft Office Excel®.

Inhibition of Self-Mediated $A\beta_{42}$ Aggregation

Amyloid-β peptide (1–42) ($A\beta_{42}$) was purchased from Sigma-Aldrich as a lyophilized powder and stored at −20 °C. The samples were treated with 1,1,1,3,3,3-hexafluoropropan-2-ol (HFIP) to avoid self-aggregation and reserved. HFIP pretreated $A\beta_{42}$ samples were resolubilized with a CH_3CN/Na_2CO_3 (300 μM)/NaOH (250 μM) (48.3 : 48.3 : 4.3, v/v/v) solvent mixture in order to have a stable stock solution. This $A\beta_{42}$ alkaline solution (500 μM) was diluted in phosphate buffer (0.215 M, pH 8.0) to obtain a 40 μM solution. Due to the hydrophobic nature of the compounds under study, they were first dissolved in methanol (1 mg/mL) and then, further diluted in phosphate buffer to a final concentration of 80 μM.

To study the $A\beta_{42}$ aggregation inhibition, a reported method, based on the fluorescence emission of thioflavin T (ThT), was followed.[22,23,30] Firstly, $A\beta_{42}$ (10 μL) samples and the tested compounds (10 μL) were diluted with the phosphate buffer to a final concentration of 40 μM (Aβ) and 80 μM (compounds), and then, they were incubated for 24 h at 37 °C, without stirring. As for the control, a sample of the peptide was incubated under identical conditions but

without the inhibitor. After incubation, the samples were added to a 96-well plate (BD Falcon) with 180 μL of 5 μM ThT in 50 mM glycine-NaOH (pH 8.5) buffer. Blank samples were prepared for each concentration in a similar way, devoid of peptide. After 5 min incubation with the dye, the ThT fluorescence was measured using a Spectramax Gemini EM (Molecular Devices) at the following wavelengths: 446 nm (excitation) and 485 nm (emission). The percent inhibition of the self-induced aggregation due to the presence of the test compound was calculated by the Eqn. 5. In which IF_i and IF_0 corresponded to the fluorescence intensities, in the presence and the absence of the test compound, respectively, minus the fluorescence intensities due to the respective blanks.

$$\% I = 100 - \left(\frac{IF_i}{IF_0} \times 100\right) \quad (5)$$

The reported values were obtained as the mean ± SEM of duplicate of two different experiments.

Acknowledgements

Authors acknowledge Jain University for financial support and A.H. is thankful to Erasmus NAMASTE consortium (unique grant number: NAMASTE_-20140147) for the award of her doctoral exchange fellowship and also the Portuguese NMR (IST-UL Center) and Mass Spectrometry Networks (Node IST-CTN) for providing access to their facilities.

Author Contribution Statement

Dr. Rangappa S. Keri: Work design and written. Dr. Asha Hiremathad: Experiment carried and written. Dr. Silvia Chaves: Modeling and biological studies.

References

[1] Alzheimer's Association, 'Alzheimer's disease facts and figures', *Alzheimer's Dementia* **2017**, *13*, 325–3732.
[2] C. C. Tan, J. T. Yu, H. F. Wang, M. S. Tan, X. F. Meng, C. Wang, T. Jiang, X. C. Zhu, L. Tan, 'Efficacy and safety of donepezil, galantamine, rivastigmine, and memantine for the treatment of Alzheimer's disease: a systematic review and meta-analysis', *J. Alzheimer's Dis.* **2014**, *41*, 615–631.
[3] J. L. Cummings, T. Morstorf, K. Zhong, 'Alzheimer's disease drug-development pipeline: few candidates, frequent failure', *Alzheimer's Res. Ther.* **2014**, *6*, 37–43.
[4] R. Jakob-Roetne, H. Jacobsen, 'Alzheimer's disease: From pathology to therapeutic approaches', *Angew. Chem.* **2009**, *48*, 3030–359.
[5] S. Chan, S. Kantham, V. M. Rao, M. Kumar, H. L. Pham, P. N. Shaw, R. P. Mcgeary, B. P. Ross, 'Metal chelation, radical scavenging and inhibition of $A\beta_{42}$ fibrillation by food constituents in relation to Alzheimer's disease', *Food Chem.* **2016**, *199*, 185–194.
[6] R. Y. Lai, C. R. Harrington, C. Wischik, 'Absence of a role for phosphorylation in the tau pathology of Alzheimer's Disease', *Biomol. Eng.* **2016**, *6*, 19.
[7] J. Berger-Sweeney, 'The cholinergic basal forebrain system during development and its influence on cognitive processes: important questions and potential answers', *Neurosci. Biobehav. Rev.* **2003**, *27*, 401–411.
[8] R. Schliebs, T. Arendt, 'The significance of the cholinergic system in the brain during aging and in Alzheimer's disease', *J. Neural Transm.* **2006**, *113*, 1625–1644.
[9] M. Pohanka, 'Alzheimer's disease and oxidative stress: a review', *Curr. Med. Chem.* **2014**, *21*, 356–364.
[10] A. I. Bush, R. E. Tanzi, 'Therapeutics for Alzheimer's disease based on the metal hypothesis', *Neurotherapy* **2008**, *5*, 421–432.
[11] C. Rodríguez-Rodríguez, M. Telpoukhovskaia, C. Orvig, 'The art of building multifunctional metal-binding agents from basic molecular scaffolds for the potential application in neurodegenerative diseases', *Coord. Chem. Rev.* **2012**, *256*, 2308–2332.
[12] M. A. Santos, K. Chand, S. Chaves, 'Recent progress in multifunctional metal chelators as potential drugs for Alzheimer's disease', *Coord. Chem. Rev.* **2016**, *327–328*, 287–303.
[13] D. S. Auld, T. J. Kornecook, S. Bastianetto, R. Quirion, 'Alzheimer's disease and the basal forebrain cholinergic system: relations to beta-amyloid peptides, cognition, and treatment strategies', *Prog. Neurobiol.* **2002**, *68*, 209–245.
[14] Z. Yan, J. Feng, 'Alzheimer's disease: interactions between cholinergic functions and beta-amyloid', *Curr. Alzheimer Res.* **2004**, *1*, 241–248.
[15] A. Hiremathad, R. S. Keri, A. R. Esteves, S. M. Cardoso, S. Chaves, M. A. Santos, 'Tacrine-Hydroxyphenylbenzimidazole hybrids as potential multitarget drug candidates for Alzheimer's disease', *Eur. J. Med. Chem.* **2018**, *148*, 255–267.
[16] PDB, entry, 1ODC. http://www.rcsb.org/pdb/explore/explore.do?structureId=1ODC.
[17] QikProp, version 2.5, Schrödinger, LLC, New York, NY, 2005.
[18] C. A. Lipinski, F. Lombardo, B. W. Dominy, P. J. Feeney, 'Experimental and computational approaches to estimate solubility and permeability in drug discovery and development settings', *Adv. Drug Delivery Rev.* **1997**, *23*, 3–26.
[19] B. Tepe, D. Daferera, M. Sökmen, M. Polissiou, A. Sökmen, '*In vitro* antimicrobial and antioxidant activities of the essential oils and various extracts of *Thymus eigii* M. Zoharyet P. H. Davis', *J. Agric. Food Chem.* **2004**, *52*, 1132–1137.
[20] G. L. Ellman, K. D. Courtney, V. J. Andres, R. M. Feather-Stone, 'A new and rapid colorimetric determination of acetylcholinesterase activity', *Biochem. Pharmacol.* **1961**, *7*, 88–90.

[21] R. S. Keri, C. Quintanova, S. Chaves, D. F. Silva, S. M. Cardoso, M. A. Santos, 'New tacrine hybrids with natural-based cysteine derivatives as multitargeted drugs for potential treatment of Alzheimer's Disease', *Chem. Biol. Drug Des.* **2016**, *87*, 101–111.
[22] M. Bartolini, C. Bertucci, M. L. Bolognesi, A. Cavalli, C. Melchiorre, V. Andrisano, 'Insight into the kinetic of amyloid beta (1–42) peptide self-aggregation: elucidation of inhibitors' mechanism of action', *ChemBioChem* **2007**, *8*, 2152–2161.
[23] X. Chao, X. He, Y. Yang, X. Zhou, M. Jin, S. Liu, Z. Cheng, P. Liu, Y. Wang, J. Yu, Y. Tan, Y. Huang, J. Qin, S. Rapposelli, 'Design, synthesis and pharmacological evaluation of novel tacrine-caffeic acid hybrids as multi-targeted compounds against Alzheimer's disease', *Bioorg. Med. Chem. Lett.* **2012**, *22*, 6498–6502.
[24] W. L. F. Armarego, D. D. Perrin, 'Purification of Laboratory Chemicals', 4th edn., Butterworth-Heinemann, Oxford, 1999.
[25] Maestro, version 9.3. Schrödinger Inc., Portland, OR, 2012.
[26] T. Hassinen, M. J. Peräkylä, 'New energy terms for reduced protein models implemented in an off-lattice force field', *Comput. Chem.* **2001**, *22*, 1229–1242.
[27] M. Clark, R. D. Cramer III, N. Van Opdenbosch, 'Validation of the general purpose Tripos 5.2 force field', *J. Comput. Chem.* **2004**, *10*, 982–1012.
[28] G. Jones, P. Willett, R. C. Glen, A. R. Leach, R. Taylor, 'Development and validation of a genetic algorithm for flexible docking', *J. Mol. Biol.* **1997**, *267*, 727–748.
[29] J. Sebestík, S. M. Marques, P. L. Falé, M. A. Santos, D. M. Arduíno, S. M. Cardoso, C. R. Oliveira, M. L. Serralheiro, M. A. Santos, 'Bifunctional phenolic-choline conjugates as anti-oxidants and acetylcholinesterase inhibitors', *J. Enzyme Inhib. Med. Chem.* **2011**, *26*, 485–497.
[30] C. Quintanova, R. S. Keri, S. M. Marques, M. G. Fernandes, S. M. Cardoso, M. L. Serralheiro, M. A. Santos, 'Design, synthesis and bioevaluation of tacrine hybrids with cinnamate and cinnamylideneacetate derivatives as potential anti-Alzheimer drugs', *MedChemComm* **2015**, *6*, 1969–1977.

Received February 4, 2020
Accepted December 21, 2020

